Contents lists available at GrowingScience

Current Chemistry Letters

homepage: www.GrowingScience.com

Theoretical anti-tuberculosis activity and molecular docking investigation of N-silylated heterocyclic compounds with benzyl chloride catalyzed by ammonium sulfate-doped red algae (AS@CRA)

Ali Barazzouq[a], Driss Ouzebla[a], Rachid Hsissou[a], Mohammed Daoudi[a], Ali H. Bahkali[b], Abdellah Zeroual[c], Shifa Wang[d], Asad Syed[b] and Mohamed El idrissi[e*]

[a]*Laboratory of Organic Chemistry, Bioorganic and Environment (LOCBE), Faculty of Science, Chouaïb Doukkali University, P.O. Box 20, 24000, El Jadida, Morocco*
[b]*Department of Botany and Microbiology, College of Science, King Saud University, P.O. Box 2455 Riyadh 11451, Saudi Arabia*
[c]*Molecular Modelling and Spectroscopy Research Team, Faculty of Science, Chouaïb Doukkali University, P.O. Box 20, 24000 El Jadida, Morocco*
[d]*School of Electronic and Information Engineering, Chongqing Three Gorges University, Chongqing, Wanzhou, 404000, China*
[e]*Team of Chemical Processes and Applied Materials, Faculty Polydisciplinary Sultan Moulay Slimane University, Beni-Mellal Morocco*

C H R O N I C L E

Article history:
Received July 14, 2024
Received in revised form
August 12, 2024
Accepted October 3, 2024
Available online
October 3, 2024

Keywords:
Calcined Red Algae (ARC)
AS@CRA catalyst
ADME study
Isoniazid
Tuberculose

A B S T R A C T

In this charge we designated a Hilbert-Johnson process by coupling of heterocyclic N-silylated with benzyl chloride at 100°C using the calcined red algae (CRA) doped with ammonium sulfate (AS), AS@CRA as a heterogeneous catalyst. The resulting examination systems, which included atomic absorption, BET methodology and X-ray diffraction (XRD), scanning electron microscopy (SEM/EDX), and Fourier transform infrared spectroscopy (FT-IR), were employed to describe these catalysts. The effect of catalyst and alkylated agent were extensively studied. This catalyst can also be recycled several times in this condensation, and lastly, we suggested a probable answer mechanism for this process. Moreover, our molecular docking investigation revealed the anti-tuberculosis potential of the synthesized compounds. Notably, the drug isoniazid exhibited higher binding energies compared to the products 2a, 2b, and 2c. Additionally, the ADME study suggests that highly efficacious synthetic compounds may possess anti-tuberculosis properties.

1. Introduction

In recent years, the study of 1H-benzimidazoles has received considerable attention[1], and also because they have pharmaceutical[2], pancreatic lipase inhibitors[3], anticancer[4] or anti-HIV[5] activities and anti-tuberculosis[6]. Alkylated N-1 Benzimidazoles are also significant intermediates on the preparation for various ionic liquids[7,8]. Thus, the synthesis of N-1 alkylated benzimidazole derivatives depends on the biological environment. Generally, N-1 alkylation of amines is obtained[9] by reaction with an alkyl halide using K_2CO_3 or anhydrous Cs_2CO_3 in DMF. The Silyl-Hilbert-Johnson reaction[10] is the most commonly used approach for the condensation of natural silylated bases and sugars to give nucleosides, based on the coupling of O, N-silylated heterocyclic, in particular of nucleic bases, and halides or sugar acetates in the presence of Friedel-Crafts catalysts[11] (for example, $SnCl_4$ or TMSOTf)). These reactions were produced with hexamethyldisilazane (HMDS) in the presence of trimethylsilyl chloride (TMSCl)[12] at reflux. Despite these available methods, we find simple and green synthesis strategies, by heterogeneous catalysis[13] which avoids the use of expensive and dangerous catalysts. Heterogeneous catalysts have advantages such as: simple handling[14], non-toxicity[15], easy separation[16], protects the environment[17] and low cost. With this in mind, we find certain heterogeneous catalysts, which are studied such as natural phosphate[18,19], zeolites[20], alumina[21] and porous carbonaceous materials[22], the latter being attractive in terms of their extent.

* Corresponding author
E-mail address m.elidrissi2018@gmail.com (M. El idrissi)

doi: 10.5267/j.ccl.2024.10.001

Surface, physicochemical domains, stability, and high availability. Additionally, they are widely used as absorbents for separation processes. In this work, we described the Hilber-Johnson process by coupling silylated benzimidazole or its silylated analogues with benzyl chloride catalyzed by red algae doped with ammonium sulfate AS@CAR as a perfect heterogeneous catalyst. The first step involves the silylation of benzimidazole or its analogues in the presence of HMDS and the second step involves adding benzyl chloride to give the desired product. (**Schema 1**)

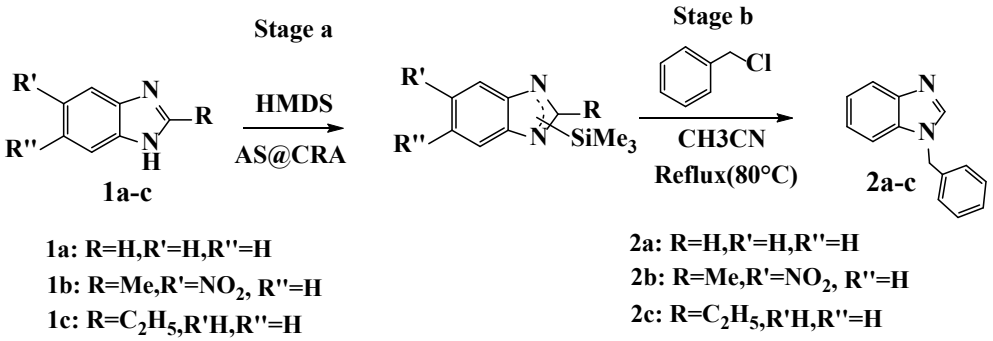

Scheme 1. General Hilbert-Johnson process

In this work we carried out the condensation of heterocyclic –N-silyl and benzyl chloride by Hilbert Johnson's process using AS@CRA as catalyst, in addition we tested the products obtained against tuberculosis by molecular docking and compared with the drug Isoniazid (**Fig. 1**), we also conducted an ADME survey of synthetic compounds

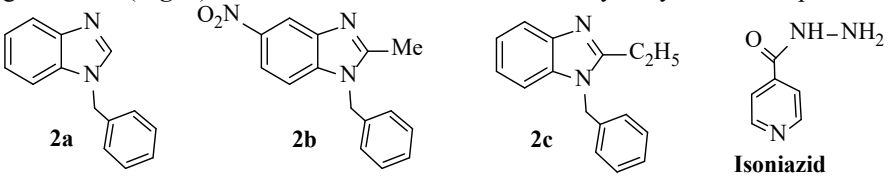

Fig. 1. Drug Isoniazid

2. Research method

2.1. Preparation of AS@CRA (3/1)

Initially, the collected red algae remaining was washed with water, dried at 70°C for 24 hours, then creased and sieved. Then calcined at 500°C for 2 hours under nitrogen to give a solid funding (RCA). The next stage includes doping these red algae with AS ($(NH_4)_2SO_4$), presenting the aqueous solution of amonium sulfate (1g) against a form of (3g) of calcined red algae and of way this assortment is moved at room temperature for 20 minutes and taken to vaporization then leaves the catalyst (AS@CRA) is parched in the oven at 100°C for 12 h.

2.2. Experimental Procedures

During this work we always based on benzimidazole as the test compound. Indeed, in a flask, we mix 1 mmol of benzimidazole 1 equivalent of AS@RCA, 2 ml of HMDS, the mixture rotates for 2 hours at reflux (100°C) until the total silylation of the heterocyclic base (solution clear) then 1 equivalent of benzylchloride and 3 ml of acetonitrile are added, the mixture is stirred overnight at 80°C.The residue is filtered, followed by liquid-liquid extraction with chloroform and water .The organic phase is dried with sodium sulfate Na_2SO_4, filtered and evaporated. Then the filtrate is purified on a silica gel column using the whole (hexane/ethyl acetate) as eluent.

Table 1. Study of catalyst effect for synthesis of **2a**

Optimal Conditions: **Stage 1:** Benzimidazole (1mmol), Catalyst AS@ CRA (1eq), **Stage 2**:CH_3CN (3 ml) Benzylchloride (1 eq), reflux reflux (100°C) for 12h

Entry	**Stage 1** In HMDS 2ml	**Stage2** In CH_3CN	Yield (%)
1	Benzimidazole	Benzylchlorid: 1eq ,AS@CRA :1eq	74
2	Benzimidazole, AS@CRA:1eq	Benzylchlorid : 1eq	**86**
3	Benzimidazole , $(NH_4)_2SO_4$: 1eq	Benzylchlorid: 1eq ,CRA :1eq	70
4	Benzimidazole,CRA:1eq	Benzylchlorid: 1eq,$(NH_4)_2SO_4$:1eq	73
5	Benzimidazole ,CRA :1eq	Benzylchlorid : 1eq	65
6	Benzimidazole ,$(NH_4)_2SO_4$ 1eq	Benzylchlorid : 1eq	56
7	Benzimidazole, $(NH)_2SO_4$:1eq + CRA :1eq	Benzylchlorid : 1eq	76
8	Benzimidazole	Benzylchlorid: 1eq $(NH_4)_2SO_4$):1eq+CRA:1eq	72
9	Benzimidazole, AS@CRA:0.75eq	Benzylchlorid : 1eq	78
10	Benzimidazole, AS@CRA:0.5eq	Benzylchlorid : 1eq	75

Table 2.Study of benzyl chloride effect for synthesis of **2a**

Entry	Stage 1 In HMDS (2ml)	Stage2 In CH_3CN	Yield (%)
1	Benzimidazole, AS@CRA:1eq	Benzylchlorid :1eq	**86**
2	Benzimidazole , **AS@CRA**:1eq	Benzylchlorid :0.75eq	**75**
3	Benzimidazole, AS@CRA:1eq	Benzylchlorid : 0.5eq	**63**

Table 3. Generalization of the method to other compounds **2a-c**

Entry	Heterocyclic compounds 2a-c	Yield (%)
1	**2a**	**86**
2	**2b**	**77**
3	**2c**	**81**

Table 4
Recycling of the catalyst (AS@CRA)

Product	Catalyst	Yield %
2a	Fresh	**86**
2a	First test	**75**
2a	Second test	**63**
2a	Third test	**56**

3. Results and analysis: Report of AS@CRA

3.1. FT-IR of RA and AS@CRA

The multitudes pulled weighed in the field from 500 to 4000cm^{-1}. Infrared spectroscopy (FT-IR) can qualitatively prove the substance edifice of the typical intended.

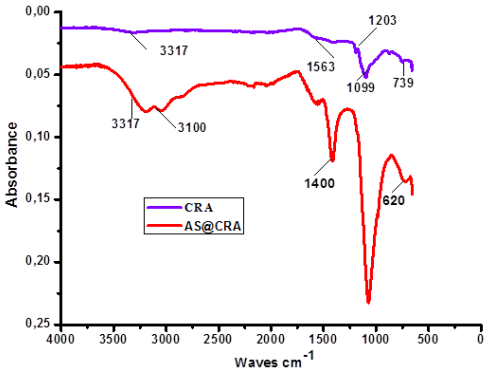

Fig. 2. FT-IR spectra of CRA, AS@CRA

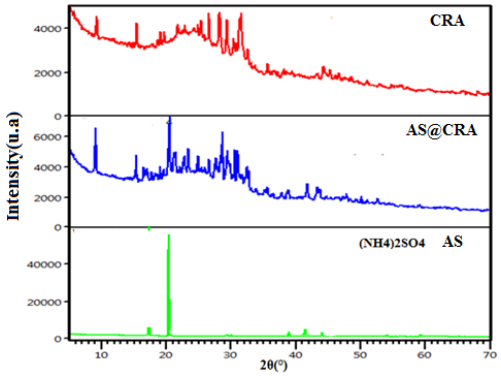

Fig. 3. XR of CRA, AS and AS@CRA

The FT-IR spectrum of RA displays the presence of a combination crew at 3317 cm^{-1} which tin stay tuned near O-H elongation convulsions of surface hydroxyl groups and some H_2O molecules adsorbed. The integration crew at 1563 cm^{-1} is tuned to the C=C elongation pulsations specific to the aromatic structure. Additionally, the strip at 1203 cm^{-1} tin stay tuned near the O-H curvature or the C-O elongation pulse of phenol, while the strip at 1099 cm^{-1} is tuned to the C-H curvature of alkyl groups. Another strip was found at about 739 cm^{-1} which can be joined to the out-of-plane curvature mode of O-H. The FT-IR spectrum of the AS@CRA catalyst shows mobile mutations due to the addition of Ammonium sulfate (AS), an intensification in the integration strip to 3317 cm^{-1} highlights the presence of H_2O molecules adsorbed during doping evolution. The elevation of ammonium was noticed by a higher intensity band at 1400 cm^{-1} as NH_4^+ bending vibration and at 3100 cm^{-1} as NH_4^+-Si-O stretching. The vibration bands located at 620 cm-1 are clearly visible in the AS@CRA and ammonium sulfate FTIR spectrum, indicating the existence of the –SO– groups.

3.2. DRX spectra of RA, AS and AS@CRA

The spectra were divergent with the D8 Advanced Bruker AXS ash machine with sharp Cu Kα emission (λ = 1.541 nm). The chords were wide in the 2θ variety from 5 to 70° with a variety of 0.06° and a variety of successive solitaires per variety. This establishment was frustrated at identifying obvious ages (obligatory eternities and dust) and pausing their photo. To do this, the acquired spectra were retained alongside the orientation spectra in the X'Pert High Score Plus software database. In **Fig. 3** the XRD spectra of CRA, AS and AS@CRA are presented, we have perceived that the spectrum of AS@CRA is the condensation of the spectrum of CRA and the spectrum of (AS), that is to say the peaks characterizing the

CRA and the peaks characterizing (AS) are present in the spectrum of AS@CRA. It can therefore be concluded that the XRD analysis explains the adsorption of ammonium sulfate (AS) on the surface of the CRA.

3.3. SEM-EDX

The decoding of the catalyst morphology and its surface was adhered and can be removed by scanning electron microscopy (SEM). The fundamental estimates were consolidated using an X-ray microanalyzer (EDX). The models were metallized using a gold metallic. Metallization confirms noble transmission to reduce load impacts. The SEM micrographs of CRA and AS@CRA are shown in the figures below. The micrographs of pure CRA show a surface with a heterogeneous structure containing accumulations of carbon of different weightings, dissipated incidentally. Various pores are also visible. On the other hand, the surface of the AS@CRA catalyst shows a change in the surface and clearly shows the impregnation of ammonium sulfate (AS) on the CRA support, and the catalyst particles are uniformly on the nanoscale.

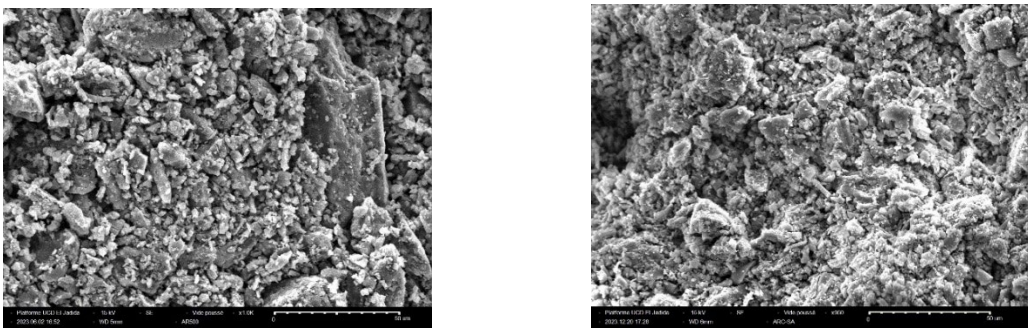

Fig. 4. SEM micrographs of CRA SEM micrographs of AS@CRA

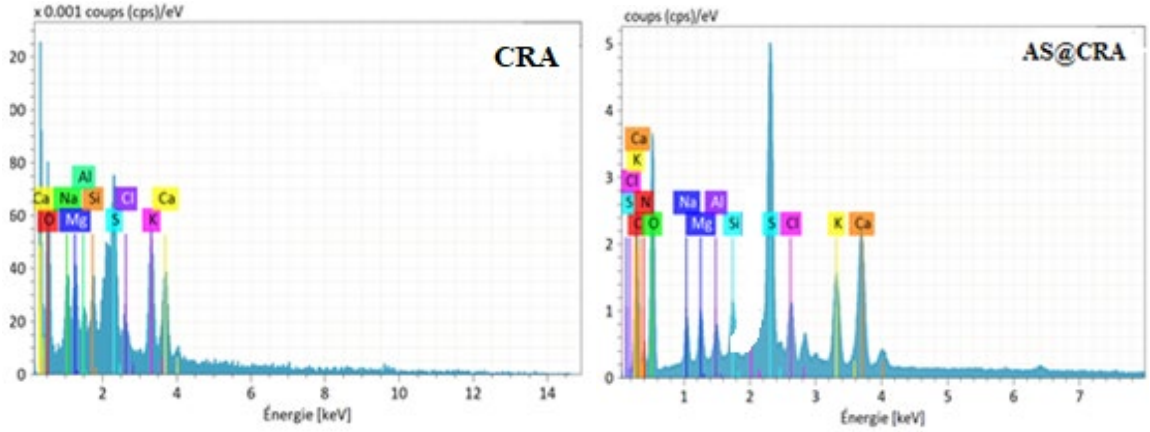

Fig. 5. EDX of CRA EDX of AS@CRA

Element determination was carried out by energy dispersive X-ray spectroscopy (EDX) for ARC and AS@CRA. For CRA the mass percentages of nitrogen, oxygen, and sulfur are 0%, 19.26% and 4.2% respectively. For AS@CRA the mass percentages have changed, for example we find 4.2% for nitrogen, 32.44 for oxygen and 5.96% for sulfur. The composition of the catalyst AS@CRA generally confirms the impregnation of ammonium sulfate AS on the ARC surface.

3.4. Catalytic study

To improve the conditions for the Hilbert Johnson reaction, AS@CRA was used as a catalyst, and a set of reactions was carried out. The reaction of benzimidazole with benzyl chloride was tested as a reference reaction. The results show that this catalyzed reaction was well responded to using for the first step: heterogeneous catalyst (AS@CRA:1eq) with HMDS and for the second step: with a yield of 86% (entry 2). Likewise, the use of the heterogeneous catalyst (AS@CRA: 1eq), benzylchloride and CH_3CN in the second step gave a yield of 74% (entry1).also in this study we worked on the influence of Amonium sulfate (AS: 1eq), (CRA: 1eq) and the mixture of (AS: 1eq and CRA: 1eq), in fact the use of (AS: 1eq) in the first step and (CRA: 1eq) in the second step gave a yield of 70% (entry 3) and also the use of (CRA: 1eq) in the first step and (AS: 1eq) in the second step gave a yield of 73% (entry3).The study also showed that the use of (CRA: 1eq) only in the first step gave a yield of 65% (entry 5) and also the use of (AS: 1eq) only in the first step gave a yield of 56% (entry 6), to compare the influence of (AS@CRA:1eq) and (AS:1eq+CRA:1eq) the results show that by using (AS:1eq+CRA:1eq) in the first step the product was obtained with a yield of 76 % (entry 7) and when (AS: 1eq + CRA: 1eq) was used in the second step the product was obtained with a yield of 72% (entry 8).

For comparison also between the number of equivalents of the AS@CRA catalyst, the product was obtained with a yield of 86% for (AS@CRA:1eq) (entry2) and with a 78% for (AS@CRA:0.75eq) (entry9) and with a yield of 75% for (AS@CRA:0.5eq) (entry10). We also studied the effect of the alkylating agent (**Table 2**) and the results show that the good yield was obtained with 86% using the equivalent of benzyl chloride. After optimizing the conditions, we applied these conditions to other heterocyclic (**Table 3**).

3.5. Recycling of the catalyst

To reading the recycled of the catalyst AS @CRA was considered to estimate the influence of the catalyst. (**Table 4**) reviews the grades of three successive catalytic tests completed under the same optimal conditions. After each reaction, the catalyst was improved by filtration, washed three times with dichloromethane and acetonitrile at a temperature of 25°C. This was done to remove all polar and nonpolar adsorbents through the reaction, then dried in an oven at 100°C and finally activated at 180°C (4 h). In **Table 6** we see that after carrying out the reaction with the fresh catalyst the product was obtained with a yield of 86%, then when the reaction was carried out under the same conditions with the catalyst recovered and activated (first test) , the product was obtained with a yield of 75%. For the second and third test, we did not observe a large variation in yield, which is of the order of (63% and 56%).

3.6. Mechanism of reaction

According to the literature, which talks about the mechanism of the reaction[23], the above mechanism could be described as follows: the first step is the silylation of benzimidazole by HMDS followed by the removal of Cl- by AS @CRA and formation of the carbocation subsequently the silylated benzimidazole reacts with the carbocation to form the desired product.

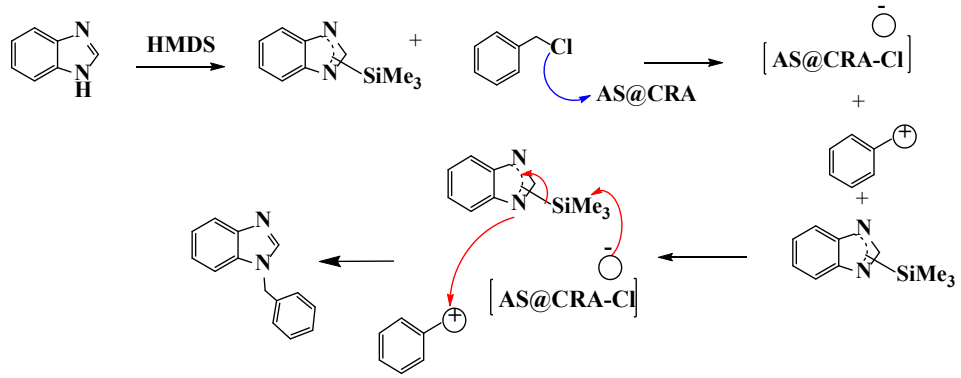

Scheme 2. Mechanism for silyl-Hilbert-Johnson reaction

❖ **^{1}H RMN , ^{13}C RMN spectra and MS Es+**

***1-benzyl-1H-benzo[d]imidazole (2a)**

Fp: 120°C
R_f: 0.3 (Hexane/ ethyl acetate, (2/1: v/v)
^{1}H NMR (600 MHz, DMSO-D6) δ 5.47 (s, 2H, CH2-N) 7.48 – 7.16 (m, 5H, C-H, Benzen) 7.48 (dd, J = 6.8Hz, C-H Benzen) 7.63 (dd, J = 6.8Hz, 2H, C-H, Benzen) 8.38 (s, 1H, C2-H)
^{13}C NMR (151 MHz, DMSO-D6) δ 111.24 (CH2-N) 122.11(C7)120.03(C5) 127.93(C6)122.92(C5) 144.12(C-CH2-N) 134.20-128.26 (5C, Benzen) 137.52(C2) 144.78(C8) 144.78(C9)
Masse: Es+=209.38.

***1-benzyl-2-methyl-5-nitro-1H-benzo[d]imidazole (2b)**

Fp: 152°C
Rf: 0.46 (Hexane/ ethyl acetate, (2/1: v/v)
^{1}H NMR (600 MHz, DMSO-D6) δ, 5.56(s, 3H, CH3). 5.63 (s, 2H, CH2) 7.24-7.2 (m, 5H, Benzen) 7.35 (m, 1H, C6-H) 7.71 (dd, J = 8.9, 7.3 Hz, 1H, C7-H) 8.42(s, 1H, C4-H)
^{13}C NMR (151 MHz, DMSO-D6) δ, 14.57 (CH3)40.57(CH2) 111.17(C8) 114.95(C9) 118.16(C2) 136.85(C7) 42.9(C6) 142.9(C51) 143.18 (C4).
Masse: Es+=268.19

***1-benzyl-2-ethyl-1H-benzo[d]imidazole (2c)**

Fp: 64°C
Rf: 0.23 (Hexane/ethyl acetate, (2/1: v/v)

^{1}H NMR (600 MHz, DMSO-D6) δ 7.55 (d, J = 7.3 Hz, 1H. C4-H) 7.42 (d, J = 7.3 Hz,1H,C7-H) 7.19 (m, 1H.C5-H)7.18(m,1H,C6-H)7.08 –7.04(m,5H, Benzen)5.45(s, 2H, CH2)2.81 (q,J =7.5 Hz,2H, CH2-CH3)1.24 (t, J = 7.5 Hz, 3H, CH3-CH2).
^{13}C NMR (151MHz), DMSO-D_6) δ.12.05(CH_3)156.67 (C2) 20.66(CH_2-CH_3) 40.59(CH_2-N) 119.01(C7) 121.81(C4) 122.22(C6) 122.91(C5) 129.29-127.03(5CBenzen) 135.99(C9) 137.69(C8) 142.86(C-CH_2-N)
Masse: Es+=236.29

3.7. Docking study

Molecular docking is a computer method that predicts the interaction between two molecules, usually a target protein and a tiny molecule called a ligand. To predict how these two molecules will bond to one another, molecular docking evaluates the interactions between their atoms. Numerous scientific domains, such as drug development, the production of novel chemical compounds, and the comprehension of molecular interactions, find use for this technique. The ligand molecule is placed within the target protein's binding site in a number of possible orientations during a standard molecular docking process. The appropriateness and affinity of these orientations are then used to rank and evaluate them. These forecasts are dependent on complex computational techniques including molecular modeling, optimization methods, and intermolecular force computations. **Table 5** present Affinity of the ligands under-study, while **Fig. 7** provide 2D and 3D interaction of the ligands with tuberculosis virus.

Table 5. Affinity in kcal/mol of the ligands derived from 1-benzyl-1H-benzo[d]imidazole compared to isoniazid.

Ligands	Affinity against tuberculosis virus (kcal/mol)
2-a	**-5.5**
2-b	**-5.8**
2-c	**-5.1**
Isoniazid	**-6.0**

Table 5 provides an overview of the affinities of different ligands towards the tuberculosis virus, measured in kcal/mol. Analysis of these data provides a better understanding of each ligand's ability to bind to the virus and potentially inhibit its activity. Negative affinity values indicate a strong interaction between the ligand and the virus, which is crucial for the development of effective TB drugs. By comparing the affinities of the various ligands with those of isoniazid, a well-known anti-tuberculosis drug, we can assess their potential as therapeutic candidates. Compared with isoniazid, ligands 2-a, 2-b and 2-c show slightly lower, but nonetheless significant, affinities. This suggests that these ligands could potentially serve as promising candidates in the development of new drugs against tuberculosis.

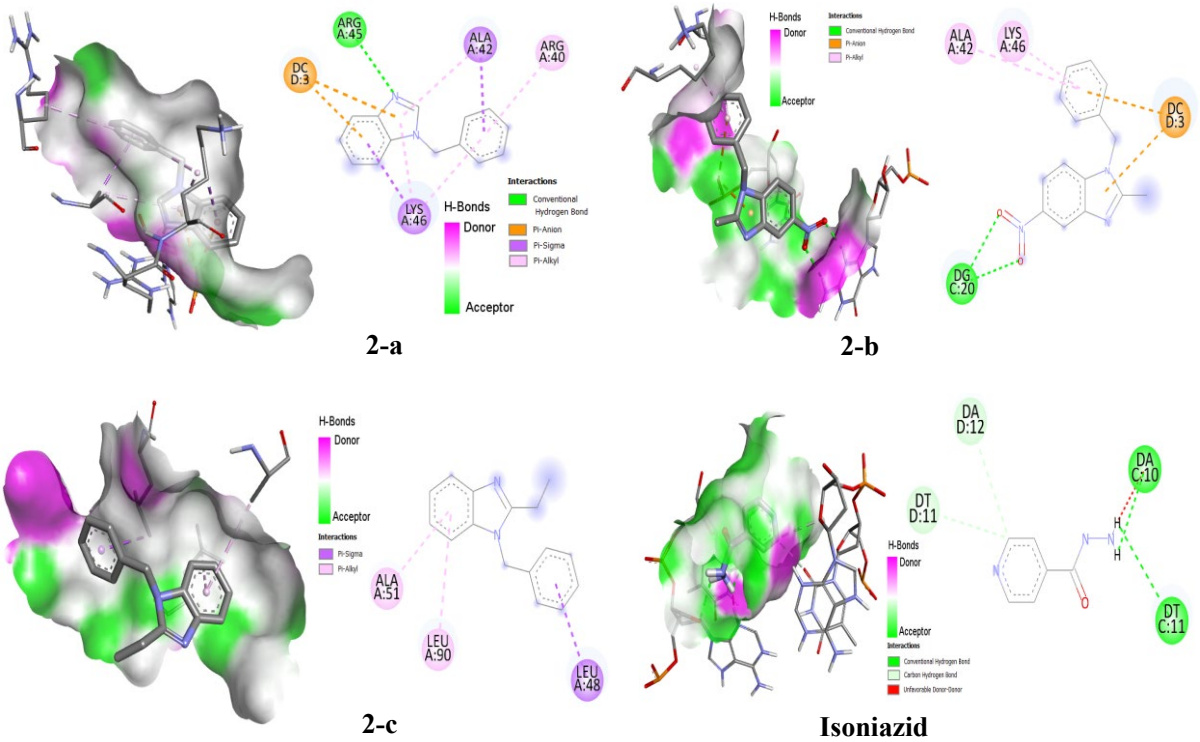

Fig. 7. 2D and 3D interaction of the ligands with tuberculosis virus

3.8. ADME study

A pivotal aspect of pharmacological investigation lies in ADME, which stands for absorption, distribution, metabolism, and elimination. The primary objective of ADME studies is to systematically explore and elucidate the intricate mechanisms governing the absorption, distribution, metabolism, and excretion of a drug from the body[24-27]. These investigations offer invaluable insights into the dynamics of drug-organ interactions and are crucial for comprehensive assessment of the safety and efficacy of a medication. They shed light on the processes involved in synthesizing and eliminating metabolites, which is indispensable for determining optimal dosages, predicting potential side effects, and maximizing therapeutic outcomes. This section provides a detailed analysis of ADME to evaluate the pharmacokinetic and pharmacodynamic properties of ligands derived from 1-benzyl-1H-benzo[d]imidazole. The aim is to offer comprehensive insights into how these substances interact with the body, furnishing vital data for assessing their potential therapeutic utility. Such information is instrumental in elucidating the pharmacological characteristics of these ligands and guiding future research endeavors aimed at utilizing them as therapeutic agents. **Fig. 6** illustrates the boiled-egg plots of the ligands under examination, while **Table 6** furnishes details on the pharmacokinetic and pharmacodynamic properties of ligands derived from 1-benzyl-1H-benzo[d]imidazole.

Table 5. Presents the pharmacokinetic and pharmacodynamic properties of ligands derived from 1-benzyl-1H-benzo[d]imidazole.

Property	2a	2b	2c	Isoniazid
Num. H-bond acceptors	1	3	1	4
Num. H-bond donors	0	0	0	1
Consensus Log $P_{o/w}$	2.79	2.37	3.43	2.26
Solubility	2.02e-03 mg/ml ; 9.71e-06 mol/l	4.48e-03 mg/ml; 1.67e-05 mol/l	3.69e-04 mg/ml; 1.56e-06 mol/l	1.42e+00 mg/ml; 6.38e-03 mol/l
Class	Moderately soluble	Moderately soluble	Moderately soluble	Soluble
GI absorption	High	High	High	High
BBB permeant	Yes	Yes	Yes	Yes
Log K_p (skin permeation)	-5.42 cm/s	-5.62 cm/s	-4.99 cm/s	-5.92 cm/s
Lipinski	Yes; 0 violation	Yes; 0 violation	Yes; 1 violation: MLOGP>4.15	Yes; 0 violation
Bioavailability Score	0.55	0.55	0.55	0.55
Synthetic accessibility	1.48	2.26	2.03	4.59

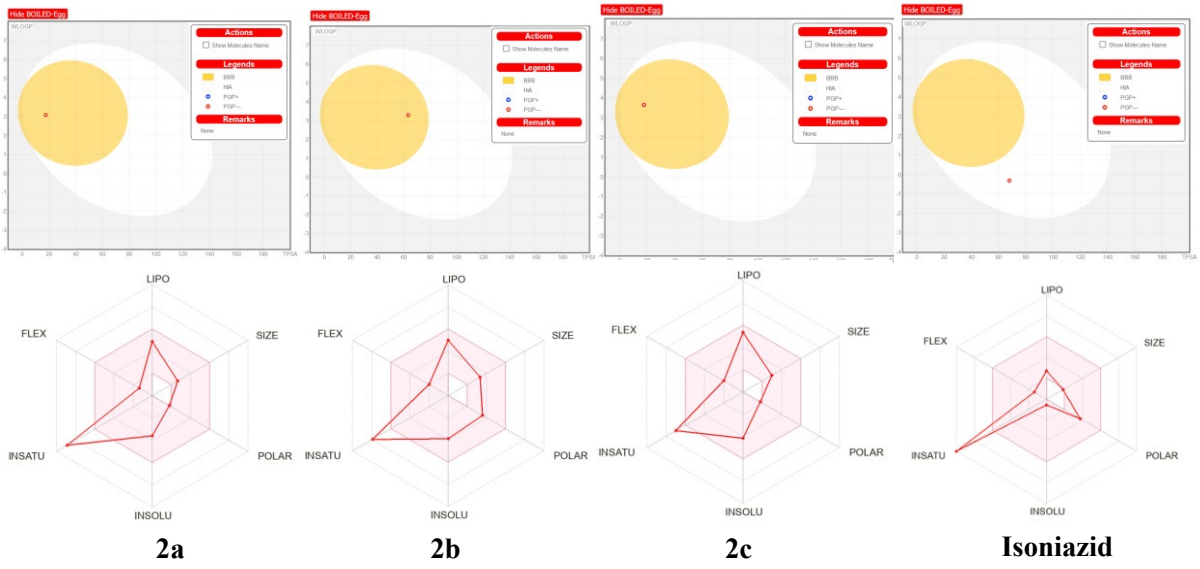

Fig. 7. Illustrates the toxicity profiles of the ligands derived from 1-benzyl-1H-benzo[d]imidazole, as evaluated by the SwissADME service.

Table 5 provides the pharmacokinetic and physicochemical properties of different compounds (2a, 2b, 2c, IS). The observations from the table are as follows:

i). Number of hydrogen bond acceptors: Compounds 2a, 2b, 2c, and Isoniazid having 1, 3, 1, and 4 hydrogen bond acceptors, respectively. This indicates the potential of each compound to form hydrogen bonds with other molecules.

ii). Number of hydrogen bond donors: Compounds 2a, 2b, 2c, and Isoniazid having 0, 0, 0, and 1 hydrogen bond donors, respectively. This may influence their ability to interact with other molecules via hydrogen bonding.

iii). Consensus Log P/o/w (octanol-water partition coefficient): This measure of lipophilicity varies between 2.26 and 3.43. The values indicate the tendency of each compound to dissolve in lipophilic or hydrophilic phases.

iv). Solubility: The solubility values range from 0.000369 mg/ml to 4.48 mg/ml, indicating the ability of each compound to dissolve in water.

v). Log Kp (skin permeation): The Log Kp values range from -5.92 cm/s to -4.99 cm/s, indicating the ability of each compound to penetrate the skin.

vi). Lipinski rule violation: Most compounds do not violate Lipinski's rule, except compound 2c, which violates one criterion (MLOGP>4.15).

vii). Synthetic accessibility: The values range from 1.48 to 4.59, indicating the ease of synthesis for each compound.

4. Conclusion

We identified a Hilbert-Johnson process in this charge by utilizing calcined red algae (CRA) doped with ammonium sulfate (AS), AS@CRA, as a heterogeneous catalyst to couple heterocyclic N-silylated with benzyl chloride at 100°C. The resulting examination systems, which included atomic absorption, BET methodology and X-ray diffraction (XRD), scanning electron microscopy (SEM/EDX), and Fourier transform infrared spectroscopy (FT-IR), were used to describe these catalysts. Numerous studies were conducted on the effects of alkylated agents and catalysts. Last but not least, we proposed a likely explanation mechanism for this process. This catalyst can also be recycled multiple times in this condensation. Furthermore, our molecular docking analysis has shown that the synthetic compounds have anti-tuberculosis potential; the drug isoniazid have higher binding energies than the 2a, 2b, and 2c products, and the ADME study indicates that highly effective synthetic compounds may have anti-tuberculosis potential.

Funding

The authors extend their appreciation to the Researchers Supporting Project number (RSP2024R15), King Saud University, Riyadh, Saudi Arabia.

Acknowledgment

The authors extend their appreciation to the Researchers Supporting Project number (RSP2024R15), King Saud University, Riyadh, Saudi Arabia.

References

1. (a) Zhilitskaya ,L.V., & Yarosh, O.N, (**2024**). The synthesis of salts of five-membered heterocyclic compounds based on N-containing cations /anions (microreview). *Chem. Heterocycl. Compd.,60* (5/6),230–232.
(b) Dubina**,** T.F., Kosarevych**,** A.V., **&** Grygorenko**,** O.O. (2024) Synthesis and reactions of novel imidazo[4,5-b]pyridine building blocks
2. Brishty, S.R., Hossain, M.J., Khandaker, M.U., Faruque, M.R.I., Osman, H., & Rahman, S.A. (**2021**) A comprehensive account on recent progress in pharmacological activities of benzimidazole derivatives. *Front. Pharmacol., 12*, 762807.
3. Hou, X.D., Guan, X.Q., Cao, Y.F., Weng, Z.M., Hu, Q., Liu, H.B., & Hou, J. (**2020**) Inhibition of pancreatic lipase by the constituents in St. John's Wort: In vitro and in silico investigations. *Int. J. Biol. Macromol., 145*, 620-633.
4. Akhtar, M.J., Yar, M.S., Sharma, V.K., Khan, A.A., Ali, Z., Haider, M.D., & Pathak, A. (2020) Recent progress of benzimidazole hybrids for anticancer potential. *Curr. Org. Chem., 27*, 5970-6014.
5. Vasava, M.S., Bhoi, M.N., Rathwa, S.K., Jethava, D.J., Acharya, P.T., Patel, D.B., & Patel, H.D. (**2020**) Benzimidazole: A milestone in the field of medicinal chemistry. *Mini-Rev. Med. Chem., 20*, 532-565.
6. Kaur, N., Bhardwaj, P., Devi, M., Verma, Y., Ahlawat, N., & Grewal P. (**2019**) Ionic liquids for the synthesis of five-membered N, N-, N, N, N-and N, N, N, N-heterocycles. *Curr. Org. Chem.*, *23*, 1214-1238.
7. Ankita, C., Sudipto, D., Tanmoy, G., Dilip, KM., & Swapan, M. (**2018**) An efficient strategy for N alkylation of benzimidazoles/imidazoles in SDS-aqueous basic medium and N-alkylation induced ring opening of benzimidazoles. *Tetrahedron, 40*, 5932-5941
8. Bhaskarjyoti, S., Rishi, R., Nimesh, R.C., Suman, M., Angshuman, R.C., & Komal, M.V. (**2023**) Highly active primary amine ligated Ru(II)-arene complexes as selective catalysts for solvent-free N-alkylation of Anilines. *Mole. Catal., 548*, 113440.
9. Elisabeth, M., Laurin, F., Christoph, K., & Ronald. (**2019**) Access to 3-Deazaguanosine Building Blocks for RNA Solid-Phase Synthesis Involving Hartwig–Buchwald C–N Cross-Coupling. *M. Org. Lett, 21*, 3900–3903.
10. Mikhail, V.M., & Marie, E.M. (2019). Syntheses and chemical properties of β-nicotinamide riboside and its analogues and derivatives. *Beilstein J. Org. Chem, 15*, 401–430.
11. Würfel, H., Kayser, M., & Heinze, T. (**2019**) Trimethylsilylation of polygalacturonic acid. *Macromol. Chem. Phys., 220*(9), 1900002.
12. Benjamin, W.J., & Lang, Xu. (**2021**) Computational Methods in Heterogeneous Catalysis. *M. Chem. Rev, 121*, 1007–1048
13. Charlotte, V., & Bert, M.W. (2022) The concept of active site in heterogeneous catalysis. *Nat. Rev. Chem., 6*, 89–11.

14. Onome, E., Abiodun, O., Charles, O.O., Victor, E., & Ebube, V.A. (**2022**) Green biodiesel based on non-vegetable oil and catalytic ability of waste materials as heterogeneous catalyst. *Energy Sources A: Recovery Util. Environ. Eff., 44*, 7432-7452
15. Yan L., Jun W., Dunru Z., Xiaoqian R., Hanqing GL. (**2008**) Heteropolyanion-Based Ionic Liquids: Reaction-Induced Self-Separation Catalysts for Esterification. *Angew. Chem., 121*, 174-177
16. Ejeromedoghene, O., Oladipo, A., Okoye, C.O., Enwemiwe, V., Anyaebosim, E.V., Olusola, M., & Adewuyi, S. (**2022**) Green biodiesel based on non-vegetable oil and catalytic ability of waste materials as heterogeneous catalyst. *Energy Sources A: Recovery Util. Environ. Eff.*, *44*, 7432-7452.
17. Ouzebla, D., Ourhriss, N., Eşme, A., El idrissi, M., & Zeroual A. (**2024**) Synthesis of some ribonucleosides derivatives and molecular docking analysis against variant corona virus omicrone. *Curr. Chem. Lett., 13*, 445-450.
18. Ouzebla, D., Ourhriss, N., Fadare, O.A., El Abdallaoui, H.E.A., & Zeroual, A. (**2023**). Efficient Synthesis of Acyclic Nucleosides by N-Alkylation Using K2CO3 Supported with Natural Phosphate (K2CO3@ NP) as Catalyst and Docking Study Against VIH. *Chem. Africa, 6*(2), 881-890.
19. Yuchao, C., Weili, D., Guangjun, W., Naijia, G., & Landong, L. (**2021**) Confinement in a Zeolite and Zeolite Catalysis, Confinement in a Zeolite and Zeolite Catalysis. *Acc. Chem. Res, 54*, 2894–2904
20. Nooshin, G., Zanjani, A., Kamran, P., & Elmira, Y. (2020) Biodiesel production in the presence of heterogeneous catalyst of alumina: Study of kinetics and thermodynamics**.** *Int. J. Chem. Kinet., 52*, 472-484
21. Sumit, H.D., Tarkeshwar, K., & Gopinath, H. (**2018**) Recent advancement and prospective of heterogeneous carbonaceous catalysts in chemical and enzymatic transformation of biodiesel. *Energy Conv. Manag, 167*, 176-202.
22. (a) Ouzebla, D., Ourhriss, N., Eşme, A., El idrissi, M., & Zeroual, A. (**2024**) Synthesis of some ribonucleosides derivatives and molecular docking analysis against variant corona virus omicrone. *Curr. Chem, Lett., 13*, 445-450(b) Chengyuan, L., Weihui, J., Shunjun, D., Han, S., & Gennian, M. (**2017**) Effective Synthesis of Nucleosides Utilizing O-Acetyl-Glycosyl Chlorides as Glycosyl Donors in the Absence of Catalyst: Mechanism Revision and Application to Silyl-Hilbert-Johnson Reaction. *Mol., 22*, 84, 2-8
23. Atif, M., Barhoumi, A., Syed, A., & El idrissi, M. (**2024**) ADME Study, Molecular Docking, Elucidating the Selectivities and the Mechanism of [4 + 2] Cycloaddition Reaction Between (E)-*N* ((dimethylamino) methylene)benzothioamide and (S)-3-acryloyl-4-phenyloxazolidin-2-one. *Mol Biotechnol,* 1-12.
24. Barhoumi A., Ryachi K., Zeroual A., & El idrissi M. (**2023**) Chromatography Scrutiny, Molecular Docking, Clarifying the Selectivities and the Mechanism of [3 + 2] Cycloloaddition Reaction between Linallol and Chlorobenzene-Nitrile-oxide. *J. Fluoresc*, 1-17.
25. Żmigrodzka, M., Sadowski, M., Kras, J., Dresler, E., Demchuk, O.M., & Kula K. (**2022**) Polar [3+2] cycloaddition between N-methyl azomethine ylide and trans-3,3,3-trichloro-1-nitroprop-1-ene. *Scientiae Radices*, *1*, 26-35.
26. Zeroual, A., Ríos-Gutiérrez, M., El idrissi, M., El Alaoui El Abdallaoui, H., & Domingo Luis, R. (**2019**) An MEDT study of the mechanism and selectivities of the [3+2] cycloaddition reaction of tomentosin with benzonitrile oxide. *Int. J. Quantum Chem., 119*, e25980.
27. Atif, M., Barhoumi, A., Syed, A., Bahkali, A.H., Chafi, M., Zeroual, A., Paray, B.A., Wang Sh., & El idrissi, M. (**2024**) ADME Study, Molecular Docking, Elucidating the Selectivities and the Mechanism of [4+ 2] Cycloaddition Reaction Between (E)-N ((dimethylamino) methylene) benzothioamide and (S)-3-acryloyl-4-phenyloxazolidin-2-one. *Mol. Biotech.,* 1-12.